

Temperature dependence of collagen fluorescence

Julian M. Menter*

Received 18th November 2005, Accepted 2nd February 2006

First published as an Advance Article on the web 15th February 2006

DOI: 10.1039/b516429j

Dermal collagens have several fluorescent moieties in the UV and visible spectral regions that may serve as molecular probes of collagen. We studied the temperature-dependence of a commercial calf skin collagen and acid-extracted Skh-1 hairless mouse collagen at temperatures from 9 °C to 60 °C for excitation/emission wavelengths 270/305 nm (tyrosine), 270/360 nm (excimer-like aggregated species), 325/400 nm (dityrosine) and 370/450 nm (glycation adduct). L-tyrosine (1×10^{-5} M in 0.5 M HOAc) acted as a “reference compound” devoid of any collagen structural effects. In general, the fluorescence efficiency of these fluorophores decreases with increasing temperature. Assuming that rate constant for fluorescence deactivation has the form $k_d(T) = k_d^0 \exp(-\Delta E/RT)$, an Arrhenius plot of $\log[(1/\Phi) - 1]$ vs. $1/T$ affords a straight line whose (negative) slope is proportional to the activation energy, ΔE , of the radiationless process(es) that compete with fluorescence. Because it is difficult to accurately measure Φ_f for collagen-bound fluorophores, we derived an approximate formula for an activation parameter, ΔE^* , evaluated from an Arrhenius-like plot of $\log 1/I_N$ vs. $1/T$, ($1/I_N$ vs. is the reciprocal normalized fluorescence intensity). Tyrosine in dilute solution affords a linear Arrhenius plot in both of the above cases. Using the known value of $\Phi_f = 0.21$ for free tyrosine at room temperature, we determined that ΔE^* is accurate to $\approx 25\%$ in the present instance. Collagen curves are non-linear, but they are quasi-linear below ~ 20 °C, where the helical form predominates. Values of ΔE^* determined from the data at $T < 20$ °C ranged from 6.2–8.4 kJ mol $^{-1}$ (1.5–2.0 kcal mol $^{-1}$) for mouse collagen and 10.3–11.4 kJ mol $^{-1}$ (2.5–2.7 kcal mol $^{-1}$) for calf skin collagen, consistent with collisional deactivation of the fluorescent state *via* thermally enhanced molecular vibrations and rotations. Above 20 °C, $\log 1/I_N$ vs. $1/T$ plots from Skh-1 hairless mouse collagen are concave-downward, suggesting that fluorescence deactivation from the denatured coil has a significant temperature-independent component. For calf skin collagen, these plots are concave-upward, suggesting an increase in activation energy above T_m . These results suggest that collagen backbone and supramolecular structure can influence the temperature dependence of the bound fluorophores, indicating the future possibility of using activation data as a probe of supramolecular structure and conformation.

Introduction

The fluorescence spectra of mammalian type I collagens are, in general, envelopes of several overlapping fluorescent bands. Virtually all dermal collagen preparations exhibit the “expected” tyrosine fluorescence with excitation/emission maxima at 270 nm and 300 nm respectively. In addition, there are other possible photolabile fluorophores that have maximum excitation/emission pairs at 270/360 nm, 325/400 nm, and 370/450 nm. Fluorescence at 360 nm (excitation maximum at 280 nm) is thought to be an excimer-like species that results from mutually interacting tyrosine residues that are in close proximity.¹ The 325/400 nm fluorescence is attributable to dityrosine,^{2–4} which could be formed photochemically² or enzymatically³ from neighboring tyrosine residues. Dityrosine fluorescence is quenched at pH = 8.7 by borate buffer.⁵ The 370/450 nm fluorescence could arise from post-translational, as well as chemical, and/or age-related modifications,^{6,7} and is *not* quenched by borate. The relative amount of each fluorophore in a given sample depends on the

conformation of the collagen backbone and on the surrounding milieu.

The relative intensity and wavelength distribution of the overall fluorescence envelope need not be the same for all collagen preparations. This is indeed the case for citrate-soluble calf skin collagen vs. acid-extracted Skh-1 hairless mouse collagen. As these collagens possess different fluorescence spectral properties, we were interested to see if these differences are reflected in their temperature dependent fluorescence properties. One might expect that the magnitude of the activation energies for the thermal processes that compete for fluorescence would depend on the polymer conformation and physical state (*e.g.* whether the protein is denatured). Activation energies can be estimated from knowledge of the temperature dependence of fluorescence coupled with pertinent photophysical data. Such data would supplement *ground state* thermodynamic and kinetic parameters that are obtained such measurements as viscosity/optical rotatory dispersion,^{8,9} NMR,⁹ and differential scanning calorimetry (DSC).^{10,11} It follows that the activation parameters obtained for calf skin and hairless mouse preparations may significantly differ from each other. It is also quite conceivable that the polymer backbone and/or 3-dimensional supramolecular structure would have a significant

Department of Medicine, Morehouse School of Medicine, 720 Westview Dr. S.W., Atlanta, GA, 30310-1495. E-mail: menterj@msm.edu

effect on the photophysical and/or photochemical processes of the collagen-bound fluorophores, relative to their unbound condition in fluid solution.

For a given fluorophore, one can calculate the activation energy, ΔE_A , for the deactivation process(es) that compete with fluorescence, provided the fluorescence quantum efficiency and its variation with temperature, $\Phi_f(T)$, are known. For collagen-bound fluorophores, the quantum yields, for the bound states are usually lower¹² than those determined for the free molecules in solution. Because of their relatively low (unknown) amounts, and given the pronounced scattering observed for collagen solutions in general, an estimation of the light absorbed by these bound fluorophores is difficult at best. Moreover, the local environment, which significantly affects the quantum efficiencies of these fluorophores, is not known.

Although the above considerations preclude a rigorous determination of the activation energies, we can easily derive an *approximate* activation energy, ΔE^* , which, in this case, is accurate to within roughly 25%, based on the fluorescence quantum yield of tyrosine ($\Phi_f = 0.21$ in solution at room temperature¹³). If the quantum yields for the bound fluorophores are close to that value, then the error in calculating ΔE^* for the other fluorophores will be similar to that of tyrosine in solution.

In this paper, we report ΔE^* for a commercial calf skin collagen and from acid-extracted from Skh-1 hairless mouse collagen for temperatures that encompass the physiological range (9–60 °C). It turns out that these values depend on the collagen preparation, state (*i.e.* native *vs.* denatured), and fluorophore probed. As Arrhenius kinetics are observed only at $T \leq ca. 20$ °C, where the helical form of the collagen samples predominate, the activation parameters reflect this temperature range.

Materials and methods

Materials

Except where otherwise noted, all chemicals were obtained either from Fisher Scientific (Norcross, GA), or Sigma-Aldrich (Saint Louis, MO). These were reagent grade, and therefore used without further purification.

Collagen samples

Acid-soluble collagen, extracted from Skh-1 hairless mice^{14,15} was further purified *via* salt-fractionation. Prior to each experiment, stock colloidal suspensions were made up at 0.5 mg ml⁻¹ in 0.5 M acetic acid (HOAc). SDS-PAGE data indicates a high degree of intramolecular cross-linking.

Citrate-soluble calf skin collagen, suitable for gelation studies, was obtained from Elastin Products (Owenville MO), either as a 10 mg ml⁻¹ solution in 0.075 M sodium citrate, pH 3.7 or as highly purified lyophilized powder. Data supplied by the manufacturer and our own electrophoresis data indicate that this sample has a high molecular weight (~1 000 000 Da). Its fluorescence spectral characteristics were similar, but not identical, to the hairless mouse sample (see below).

Chromatography on Biogel P2 confirmed that the various fluorescence bands (see below) were not due to low MW impurities.

All collagen samples were kept at 4 °C prior to fluorescence analysis.

Tyrosine solutions

Tyrosine was dissolved at 1×10^{-5} M in 0.5 M HOAc. This served as a “reference” compound, since its fluorescence quantum efficiency at room temperature is known.¹³ Comparison of tyrosine’s activation parameters with those obtained for each collagen sample (see below) also enables assessment of effects due to the collagen backbone on these parameters.

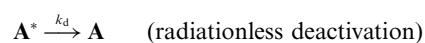
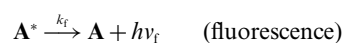
Analytical

Absorption spectra were measured on an Agilent Technology spectrophotometer at room temperature. Fluorescence emission spectra of collagen samples were recorded on a Perkin-Elmer 650–40 fluorescence spectrometer, equipped with a thermostatted sample compartment, in conjunction with a circulating bath (Lauda, K-2R; Brinkmann Instruments, Westbury, NY, USA). Horizontal entrance and exit slits in the sample compartment allow measurement of as little as 0.3 ml, and optimize measurement of turbid solutions. Optical quartz 1.0 cm cells (Hellma Cells, Inc Plainview, NY, USA) were used to collect fluorescence emitted at right angles to the excitation beam. Because of the weak fluorescence, the band widths of both excitation and emission monochromators were set at 5 nm. Fluorescence spectra were recorded at a rate of 60 nm min⁻¹. The time constant was 2.0 s. All spectra were corrected for instrumental distortion.

For temperature dependence measurements, the samples were equilibrated at 8 °C, and their fluorescence intensities were recorded at the following excitation/emission wavelengths: 270/300 nm, 270/360 nm, 325/400 nm, and 370/450 nm. Following equilibration, the temperature was slowly raised to *ca.* 60 °C at 0.4–2 °C min⁻¹. Fluorescence intensities were measured every 1–3 °C. To minimize possible collagen photodamage, the cuvettes were filled to 3.0 ml so that roughly 90% of the solution was not exposed to the excitation radiation. Exposure was kept at a minimum. Under the conditions of this study, no appreciable fluorescence fading was detected. For tests of reversibility or hysteresis, the melted collagen was slowly or rapidly cooled back down to 10–15 °C, and intensities were measured as before. A calibrated thermistor thermometer (Bailey Instruments, Saddle Brook, NJ, USA) continuously monitored temperature in the sample cuvette (Hellma Cells, Plainview, NY, USA). Control experiments established that the rate of solvent evaporation was *ca.* 3% h⁻¹ at 60 °C.

Data analysis

A simple kinetic scheme was assumed:



Molecule **A** absorbs a photon to yield excited **A***. Excited **A*** can either emit fluorescence (k_f), or undergo radiationless deactivation (k_d represents a sum of 1st order rate constants corresponding

to internal conversion, intersystem crossing, photochemical reaction(*s*), and other processes that may quench fluorescence).

If the fluorescence quantum yield, $\Phi_f(T)$, is equal to $k_r/(k_r + k_d)$, and k_d is temperature-dependent, having the form $k_d(T) = k_d^\circ \exp(-\Delta E_A/RT)$, then we have:

$$\log[(1/\Phi_f(T)) - 1] = -\Delta E_A/2.3RT + \log(k_d^\circ/k_r) \quad (1)$$

where ΔE_A represents an activation energy for collective non-radiative, temperature-dependent deactivation of the fluorescent state. A plot of $\log[(1/\Phi_f(T)) - 1]$ vs. $1/T$ should thus afford a straight line with slope $-\Delta E_A/2.3R$. The fluorescence of tyrosyl residues, and presumably the other bound fluorophores, can be quenched in a variety of ways,¹² so that one might, in general, expect these fluorophores to have a lower (unknown) fluorescence yield than their free counterparts. Thus, eqn (1) cannot be used to compute values of ΔE_A for our collagen samples. We therefore used an approximation of eqn (1), valid at low values of $\Phi_f(T)$, (eqn (2)):

$$\log 1/I_N(T) = -\Delta E^*/2.3RT + \log B \quad (2)$$

where $1/I_N(T)$ is the measured normalized fluorescence intensity at temperature, T/K , and B is a constant. The value of I_N is related to Φ_f via an unknown proportionality constant (lumped into the $\log B$ term in eqn (2)). The error arising from neglect of the $[-1]$ term in the argument of the logarithmic term increases as the fluorescence efficiency increases. In the case of tyrosine in solution, this error is $\sim 25\%$ (see Fig. 4 and discussion section). Assuming that collagen binding lowers the quantum yield, the error would be even less for collagen-bound fluorophores. Normalizing the fluorescence intensity changes the intercept, B , but has no effect on the value of ΔE^* .

Results

A: Absorption and fluorescence spectra

As shown in Fig. 1, a turbid suspension of Skh-1 hairless mouse collagen (0.5% in 0.5 M HOAc) affords an absorption spectrum that is obscured by significant light scattering. The result is a

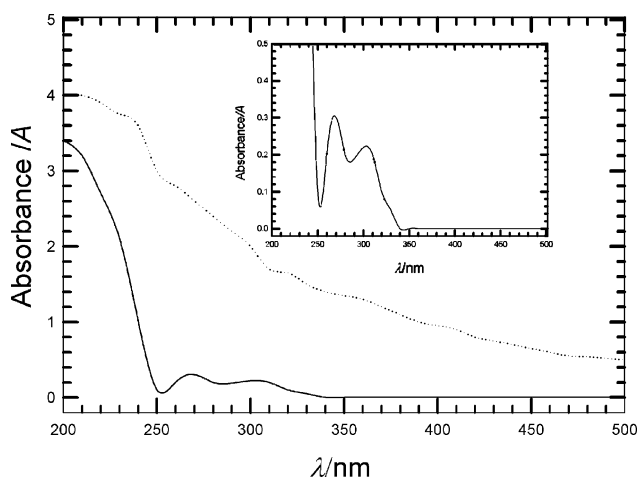


Fig. 1 Absorption spectra of Skh-1 acid-extracted collagen (dotted line) and citrate-soluble calf skin collagen (solid line) (0.25 mg ml^{-1} in 0.05 M HOAc). Inset: ordinate amplified 10-fold.

rather structureless scattering curve on which a superimposed faint absorption spectrum can be discerned at with maxima at *ca.* 240 (sh. 250–300 nm), 320 nm, 355 nm, and 410 nm. The calf skin collagen has significantly less turbidity, and yields an absorption spectrum that has a shoulder at 240 nm and low-intensity bands at 265 nm and 305 nm (sh. 325 nm) and a very faint peak at *ca.* 350 nm (see Fig. 1).

The normalized corrected fluorescence excitation and emission spectra of these samples are shown in Fig. 2(a) and (b). On excitation at 270 nm, the emission spectrum of the mouse collagen shows an apparent maximum at *ca.* 320–330 nm, shoulders at *ca.* 315 nm and 350–360 nm. The excitation spectrum of the 300 nm emission reveals a peak at 270 nm, characteristic of tyrosine. Excitation at 285 nm broadens the envelope, and increases the 360 nm fluorescence. The excitation spectrum of the 360 nm fluorescence affords a maximum at 285 nm, and is broader than the tyrosine spectrum (Fig. 2(a)). Our previous work indicates that the emission at 360 nm is probably due to an “excimer-like” species,¹ occurring as a result of interaction between two bound tyrosine molecules in close mutual proximity. Excitation at 325 nm (Fig. 2(b)) affords a maximum at *ca.* 390–400 nm. Its spectral and photochemical characteristics^{1,2} and our observation (not shown) that borate buffer can quench its fluorescence⁵ at pH 8.7 is strong evidence that this band derives from *dityrosine*. Excitation at 370 nm reveals an additional broad fluorescence band ($\lambda_{\text{max}} = 450\text{--}460 \text{ nm}$) that is not quenched by borate buffer. This fluorescence can be attributed to one or more *advanced glycation end products*.^{6,7} Excitation of 325 nm fluorescence yields a peak at 270 nm. Excitation of 430 nm fluorescence affords peaks at 285 nm and 325 nm (Fig. 2(b)). Given the marked scattering of these solutions, there is reasonable agreement between these excitation spectra and the absorption maxima in Fig. 1.

Excitation of type I calf skin citrate-soluble collagen at 270 nm, affords a fluorescence maximum at 300 nm (attributable to tyrosine), with a small shoulder at 360 nm. Excitation at 285 nm shifts the apparent maximum to *ca.* 315 nm, and increases the emission at 360 nm. The excitation spectrum of 300 nm shows a peak at *ca.* 295 nm, with a shoulder at 270 nm (tyrosine). The excitation spectrum of the 360 nm fluorescence is broadened in comparison (Fig. 3(a)). Excitation at 325 nm affords a peak at 400 nm, with a broad shoulder at 450 nm (solid line). Excitation at 370 nm affords a maximum at 450 nm. The intensity of the latter bands is very low in the calf skin collagen. The excitation spectrum for 400 nm fluorescence shows poorly resolved peaks at 275, 285, and 295 nm, as well as a broad structureless band with $\lambda_{\text{max}} \sim 325 \text{ nm}$. Excitation of fluorescence at 450 nm gives rise to an intense band at 265 nm and a less intense maximum at *ca.* 360 nm (Fig. 3(b)).

B: Temperature dependence of fluorescence

1. Tyrosine. Because tyrosine is unbound and has a well-known fluorescence yield, we could assess the accuracy of eqn (2) by comparison with eqn (1). Fig. 4 shows the temperature dependence of tyrosine fluorescence ($\lambda_{\text{ex}} = 270 \text{ nm}$; $\lambda_{\text{em}} = 300 \text{ nm}$) in 0.5 M HOAc. The fluorescence intensity decreases monotonically with increasing temperature, in accord with previous results.¹⁶ We obtained straight lines with *both* eqn (1) and eqn (2). Using $\Phi_f = 0.21$ at 300 K, we calculated $\Delta E_A = 9.08 \pm 1.30 \text{ kJ mol}^{-1}$

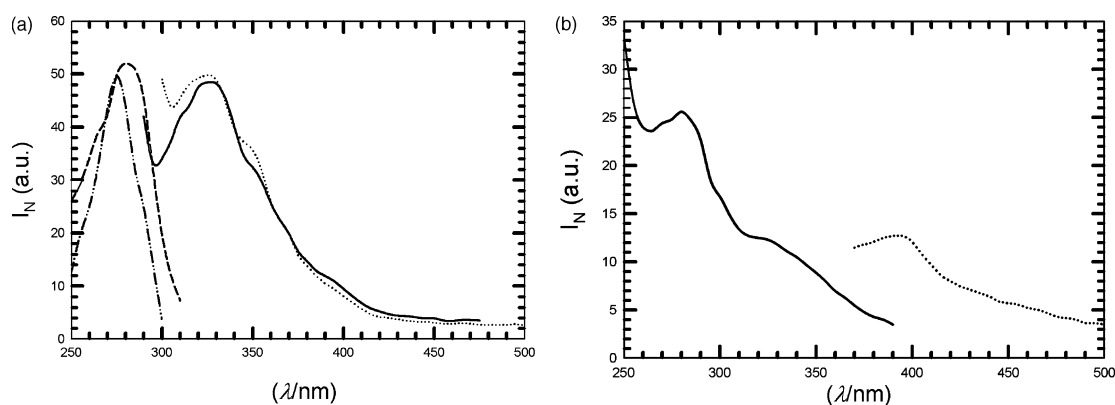


Fig. 2 (a) Fluorescence excitation and emission spectra of Skh-1 acid-soluble hairless mouse collagen (0.25 mg ml^{-1} in 0.05 M HOAc). Solid line: fluorescence excited at 270 nm ; dotted line: fluorescence excited at 285 nm ; dot dashed line: excitation of 300 nm fluorescence; dashed line: excitation of 360 nm fluorescence. (b) Fluorescence excitation and emission spectra of Skh-1 acid-soluble hairless mouse collagen (0.25 mg ml^{-1} in 0.05 M HOAc). Dotted line: fluorescence excited at 325 nm ; solid line: excitation of 430 nm fluorescence. Excitation of fluorescence at 450 nm gave rise to a very weak band at *ca.* 370 nm .

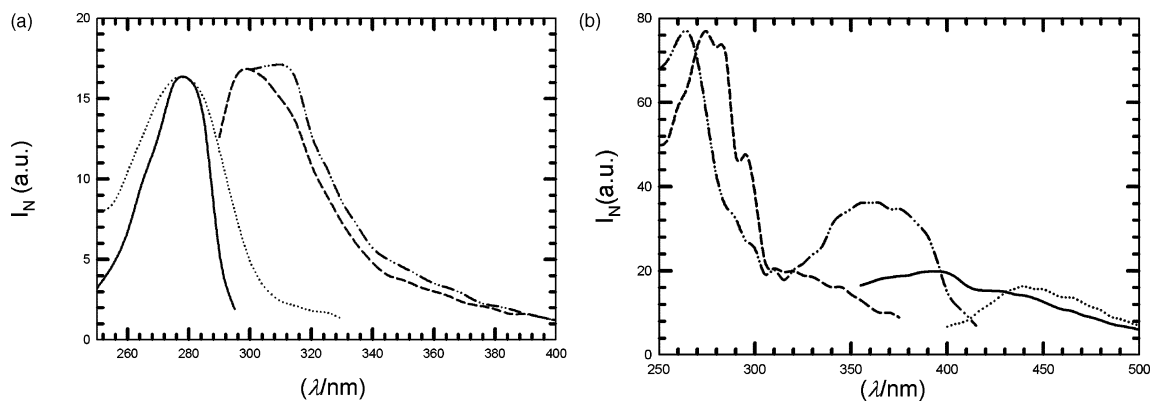


Fig. 3 (a) Fluorescence excitation and emission spectra of citrate-soluble calf skin collagen (0.25 mg ml^{-1} in 0.05 M HOAc). Dashed line: fluorescence excited at 270 nm ; dot dashed line: fluorescence excited at 285 nm ; solid line: excitation of 300 nm fluorescence; dotted line: excitation of 360 nm fluorescence. (b) Fluorescence excitation and emission spectra of citrate-soluble calf skin collagen (0.25 mg ml^{-1} in 0.05 M HOAc). Solid line: fluorescence excited at 325 nm ; dotted line: fluorescence excited at 370 nm ; dashed line: excitation of 400 nm fluorescence; dot dashed line: excitation of 450 nm fluorescence.

Table 1 Temperature dependence of tyrosine fluorescence in 0.5 M acetic acid as calculated from eqn (1) and eqn (2)

| Excitation/emission max. (λ/nm) | $\Delta E^*/\text{kJ mol}^{-1}$ (kcal mol^{-1}) |
|--|--|
| $270/300^a$ | 9.1 ± 1.9 (2.2 ± 0.3) |
| $270/300^b$ | 6.8 ± 1.3 (1.6 ± 0.1) |

^a ΔE^* determined from eqn (1). ^b ΔE^* determined from eqn (2).

($2.17 \pm 0.31 \text{ kcal mol}^{-1}$) with eqn (1), whereas eqn (2) afforded a value of $6.82 \pm 0.96 \text{ kJ mol}^{-1}$ ($1.63 \pm 0.23 \text{ kcal mol}^{-1}$) for ΔE^* (mean \pm SD of three measurements), as are shown in Table 1. Thus, for tyrosine, the mean error arising from use of eqn (2) instead of eqn (1) is $[\Delta E_A - \Delta E^*]/\Delta E_A = 25\%$.

2: Skh-1 hairless mouse and calf skin collagens. Representative comparative data are shown in Fig. 5 and 6 for each excitation/emission pair. Arrhenius plots of $\log 1/I_N$ vs. $1/T$ are non-linear, although straight lines can be “forced” through these data, in some cases. All of these curves are better fitted to a 2nd

order regression line. However, at temperatures sufficiently below T_m , where the helical form predominates (*ca.* $20 \text{ }^\circ\text{C}$), the plots are quasi-linear, allowing estimation of activation energies in this region (see insets to Fig. 5 and 6). Values of ΔE^* (mean \pm SD) are given in Table 2 ($n = 3$).

For *calf skin collagen* (Fig. 5), mean values of ΔE^* are 11.4 , 10.5 , and 10.3 kJ mol^{-1} (2.7 , 2.5 , and $2.5 \text{ kcal mol}^{-1}$) for excitation/emission pairs at $270/300$, $270/360$ and $370/450 \text{ nm}$, respectively. Measurements of $325/400 \text{ nm}$ and of $370/450 \text{ nm}$ fluorescence are subject to considerable uncertainty owing to the low fluorescence intensities and the pronounced concavity even at lower temperatures. Owing to the low fluorescence intensities of the latter bands, we were not able to obtain meaningful activation data for $325/400 \text{ nm}$ fluorescence, and the data at $370/450 \text{ nm}$ are subject to large uncertainties.

For *Skh-1 hairless mouse collagen* (Fig. 6), mean values of ΔE^* are 6.2 , 7.3 , 8.4 , and 7.5 kJ mol^{-1} (1.5 , 1.7 , 2.0 and $1.8 \text{ kcal mol}^{-1}$) for excitation/emission pairs at $270/300$, $270/360$, $325/400$, and $370/450 \text{ nm}$, respectively. Fluorescence intensities at $325/400$ and $370/450 \text{ nm}$ are roughly 10 and 4 times respectively greater

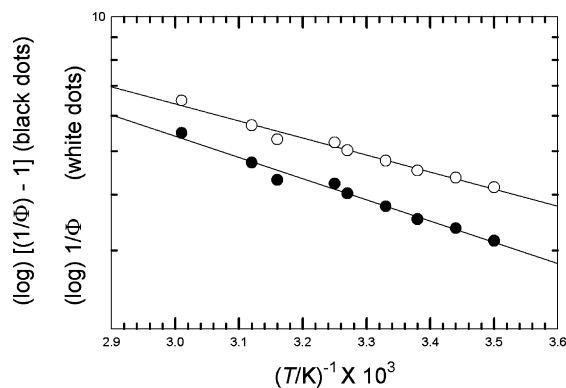


Fig. 4 Error in activation energy resulting from use of eqn (2) instead of eqn (1) for 5×10^{-5} M tyrosine in 0.05 M HOAc (see text). Excitation wavelength: 270 nm; emission wavelength: 300 nm. Black circles: use of eqn (2); $\Delta E^* = 6.82 \text{ kJ mol}^{-1}$ ($1.63 \text{ kcal mol}^{-1}$). White circles: use of eqn (1) $\Delta E_A = 9.08 \text{ kJ mol}^{-1}$ ($2.17 \text{ kcal mol}^{-1}$). Mean error in measurement = $[\Delta E_A - \Delta E^*]/\Delta E_A = 25\%$ for tyrosine, $\Phi_f = 0.21$. The error is inversely proportional to the fluorescence quantum yield. Operationally, eqn (1) is valid for fluorophores with $\Phi_f \leq 0.1-0.3$.

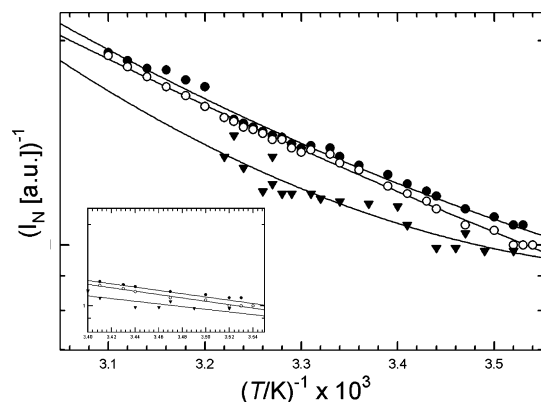


Fig. 5 Temperature dependence of normalized citrate-soluble calf skin collagen fluorescence (0.25 mg ml^{-1} in 0.05 M HOAc). Black circles: excitation at 270 nm, emission at 300 nm; white circles: excitation at 270 nm, emission at 360 nm; black triangles: excitation at 370 nm, emission at 450 nm. Data fit to 2nd order linear regression. Inset: data at $T < 20^\circ\text{C}$, fit to 1st order linear regression. Values of ΔE^* in Table 2 are calculated from this part of the melting curve.

than their counterparts in the calf skin preparation, so that the uncertainty of measurement was much smaller.

Inspection of the melting curves for calf skin and hairless mouse collagens plots reveals striking differences in behavior. Calf skin collagen curves are concave upward, whereas the mouse collagen curves are concave downward. In the calf skin sample, the

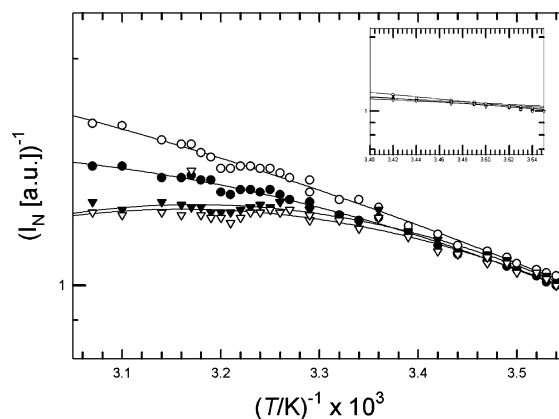


Fig. 6 Temperature dependence of normalized acid-extracted Skh-1 collagen fluorescence (0.25 mg ml^{-1} in 0.05 M HOAc). Black circles: excitation at 270 nm, emission at 300 nm; white circles: excitation at 270 nm, emission at 360 nm; black triangles: excitation at 370 nm, emission at 450 nm; white triangles: excitation at 325 nm, emission at 400 nm. Data fit to 2nd order linear regression. Inset: data at $T < 20^\circ\text{C}$, fit to 1st order linear regression. Values of ΔE^* in Table 2 are calculated from this part of the melting curve.

normalized curves are very similar to each other. In hairless mouse collagen, on the other hand, the departure from linearity increases in the order $270/360 < 270/300 \text{ nm} < 325/400 \sim 370/450 \text{ nm}$. The latter two curves appear to flatten out above 300 K.

3: On the reversibility of collagen melting. Melted collagens that are slowly cooled back to 10°C reveal signs of hysteresis, similar to that observed by Leikina *et al.*¹¹ (Fig. 7(a) and (b)). This effect ($\leq 10\%$ loss of fluorescence intensity) was also observed when the melted samples were suddenly cooled to 15°C . Although cooling increases the fluorescence intensities, they do not reach their original values, creating the appearance of an irreversible process. We did not equilibrate our samples sufficiently long (~ 10 days or more¹¹) to test whether this is the case, or whether we deal with a truly reversible but very slow equilibrium.

Discussion

We have studied the temperature dependence of collagen fluorescence in two different samples, namely acid-soluble extracted collagen from Skh-1 hairless mice and a commercial citrate-soluble calf skin collagen. We have calculated a parameter, ΔE^* that, at moderate fluorescence yields, is a reasonable approximation for the activation energy, ΔE_A , of the fluorescent state. ΔE^* (approximately) represents thermal energy needed for excited collagen molecules to reach a crossing point on the excited

Table 2 Temperature dependence of citrate-soluble calf skin and of Skh-1 hairless mouse collagen fluorescence below the denaturation temperature

| Excitation/emission max. (λ/nm) | ΔE^* (Skh-1)/ kJ mol^{-1} (kcal mol^{-1}) | ΔE^{*a} (calf skin)/ kJ mol^{-1} (kcal mol^{-1}) |
|--|---|--|
| 270/300 | 6.2 ± 1.1 (1.5 ± 0.23) | 11.4 ± 0.9 (2.7 ± 0.2) |
| 270/360 | 7.3 ± 1.5 (1.7 ± 0.4) | 10.5 ± 0.3 (2.5 ± 0.1) |
| 325/400 | 8.4 ± 1.5 (2.0 ± 0.4) | ^b |
| 370/450 | 7.5 ± 1.6 (1.8 ± 0.4) | 10.3 ± 1.7 (2.5 ± 0.4) |

^a ΔE^* determined from slopes of first order regression lines according to eqn (2) (see text; $n = 3$). ^b Fluorescence is too weak for data to be reliable.

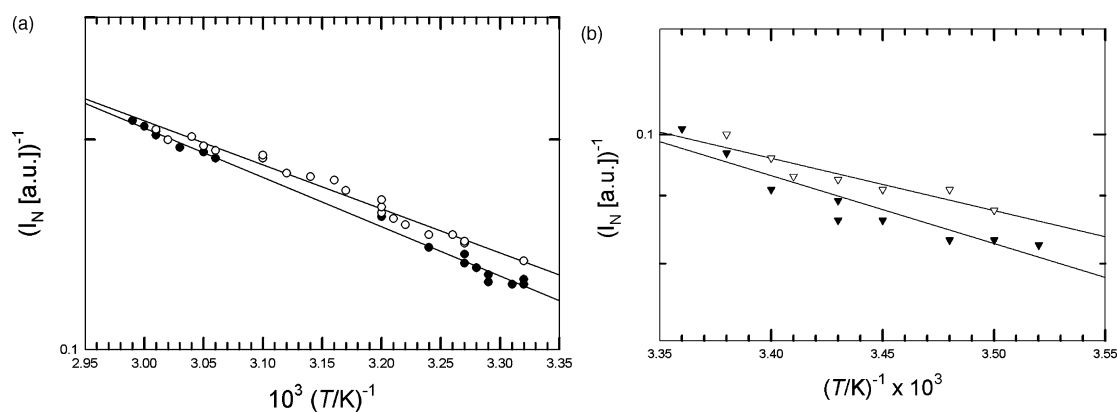


Fig. 7 (a) Hysteresis of citrate-soluble calf skin collagen melting curves. Collagen samples that had been slowly heated from 10–12 °C at 0.4–2.0 °C min⁻¹ (black dots) were cooled at similar rates (white dots). Fluorescence was recorded as described in the text. Only the data for excitation at 270 nm, emission at 300 nm are shown here for clarity. Similar behavior was observed at the other excitation/emission settings. (b) Hysteresis of Skh-1 hairless mouse collagen melting curves. Collagen samples that had been slowly heated from 10–12 °C at 0.4–2.0 °C min⁻¹ (black dots) were cooled at similar rates (white dots). Fluorescence was recorded as described in the text. Only the data for excitation at 270 nm, emission at 300 nm are shown here for clarity. Similar behavior was observed at the other excitation/emission settings.

state potential energy surface, where they can either undergo radiationless deactivation or revert back to the lowest vibrational level of the fluorescent state. In the simplest case, one observes a linear relationship between $1/[\Phi_f - 1]$ and $1/T$ (K⁻¹). For moderate fluorescence yields, as is the case for tyrosine ($\Phi_f = 0.21$), a $1/\Phi_f$ vs. $1/T$ (K⁻¹) plot also leads to a straight line, with ~25% error when the $[-1]$ term is neglected. On the other hand, Arrhenius plots did not afford straight lines for either calf skin or hairless mouse collagen fluorescence. However, at temperatures below *ca.* 20 °C, these collagens exist predominantly in the helix conformation. Here, an approximately linear Arrhenius plot is obtained, and the activation energies computed from this region have an unambiguous physical meaning.

At temperatures, where the coil to helix ratio is appreciable, the non-linearity of the melting curves could be due to several factors. The simplest explanation is that the coiled conformation(s) have different activation energies than the helix. However, it is also possible that the fluorescence quantum yield of bound fluorophores is conformation-dependent, and that $\Phi_f(T)$ is different in the coil than it is in the helix. The observation of fluorescence hysteresis suggests that such could be the case here, since hysteresis is not observed for tyrosine itself. Alternatively, it is known that collagen exhibits absorption hyperchromicity at 227 nm on denaturation.¹⁷ Because of the low chromophore extinction at the wavelengths studied here, changes in molar absorptivity would hardly be detected, but they would certainly alter the observed fluorescence intensities. At present, we cannot assess the relative effect (if any) of these factors on the fluorescence efficiency.

The shapes of the melting curves for each species differ from each other. Those for calf skin collagen are concaved upward whereas those for hairless mouse collagen tend to flatten out above the denaturation temperature. This latter effect, most pronounced for the 325/400 and 370/450 nm pairs implies that an appreciable part of the radiationless deactivation is temperature-independent,¹⁸ especially above the denaturation temperature. This is not unexpected, since our simple kinetic analysis lumped all of the non-fluorescent radiationless processes into one generic rate constant, k_d . For tyrosine, intersystem crossing to the triplet state

is essentially temperature independent from 5 to 85 °C,¹⁶ and this process could play a major role in the radiationless deactivation of denatured mouse collagen.

On the other hand, we obtain steeper curves with denatured calf skin collagen. This implies that more work must be done to attain the transition state in denatured collagen than in the native form, and that temperature-independent deactivation processes are less important here. The higher ΔE^* values found for the calf skin samples may be rationalized by assuming a different transition state geometry in the calf skin collagen than in the hairless mouse sample, possible through polymeric back-bone induced perturbations in the potential energy curves

Our values of ΔE^* for the helical form (6.3–14.6 kJ mol⁻¹; 1.5–3.5 kcal mol⁻¹), correspond to 650–1530 cm⁻¹, (based on 25% correction), consistent with activation of vibrational/rotational modes. Bowen and Sahu¹⁸ obtained similar activation energies for a series of 9-substituted anthracenes. On the other hand, they found that 1,5-dichloroanthracene afforded an activation energy of only 1.1 kJ mol⁻¹ (480 cal mol⁻¹), attributable¹⁸ to a significant temperature-independent component of fluorescence deactivation.

Besides internal conversion and intersystem crossing, other processes that compete with fluorescence include photochemical reaction(s), and quenching by adventitious molecules, *e.g.* molecular O₂. Although we have not explicitly considered photochemical processes in this work, our earlier studies indicate that most of these fluorophores are in fact photolabile,¹ and that the temperature dependence of their photochemistry should be studied in its own right. Preliminary work by us indicates, however, that collagen fluorescence is not significantly influenced by the presence of molecular O₂.

To get around some formidable experimental difficulties, we used eqn (2) as an approximate form of eqn (1). Most importantly, a rigorous thermodynamic analysis requires knowledge of the fluorescence quantum yield. Such knowledge is problematic when the fluorophores in question are attached to large biological macromolecules such as collagen for several reasons. Firstly,

alterations in the microenvironment of each bound fluorophore renders hazardous the extrapolation of photophysical data obtained from simple solutions of the fluorophore(s). Electronic effects due to nearby peptide substituents can result in fluorescence quenching.¹² In addition, our fluorescence data indicates direct tyrosine–tyrosine interaction. The latter interaction quenches tyrosine monomer fluorescence, with concomitant build-up of the 270/360 nm band.¹ Direct tyrosine–tyrosine interaction is feasible in collagen, since virtually all tyrosine residues are in the non-helical telopeptide regions.¹⁹ Our data indicate that the 3-dimensional superstructure of the mouse collagen is more favorable for this type of interaction than is that of the calf skin preparation.

Optical scattering and overlapping optical spectra further complicate matters. As can be seen from Fig. 1, there is significant light scattering, especially in the hairless mouse collagen. This makes the measured absorbance meaningless for the mouse collagen, and renders the accuracy of the measured absorbance (0.2–0.3 for the long wavelength bands) uncertain for calf skin collagen. The geometry of our fluorescence apparatus ensures that a relatively large percentage of the fluorescence is detected by the photomultiplier tube. This tends to minimize but not totally eliminate all types of light scattering by turbid biological samples. At lower temperatures, there is a tendency toward molecular aggregation, with consequent increase in turbidity. This phenomenon may be responsible for the increased scatter observed in some of the Arrhenius plots at low temperatures. Light scattering, as well as low fluorophore concentration and absorption spectral overlap from other absorbing chromophores make it impossible to accurately determine the absorbance of the fluorescent chromophore at the excitation wavelength(s).

For all of these reasons, accurate determination of fluorescence quantum yields in collagen-bound fluorophores is virtually impossible. Fortunately, for molecules with low to moderate fluorescence yields, we can obtain reasonably accurate activation data *via* eqn (2), which only requires knowledge of the fluorescence intensity and not the fluorescence quantum yield. The implicit assumption is that the unknown proportionality constant between $I_f(T)$ and $\Phi_f(T)$ does not change with temperature (*i.e.* that $I_f(T)/\Phi_f(T)$ is constant). This is a safe assumption for unbound tyrosine, in which simple Arrhenius kinetics are observed. It may not be the case for our collagen-bound fluorophores, which do not exhibit simple Arrhenius kinetics.

We compared the two methods by studying the temperature dependence of tyrosine in solution. With $\Phi_f(T) = 0.21$ at room temperature, the error in estimating the activation energy by neglecting the $[-1]$ term in eqn (2) is roughly 20%. Because of the inverse relationship between fluorescence and radiationless deactivation, this error increases as $\Phi_f(T)$ increases. As $\Phi_f(T) \rightarrow 1$, the error becomes very large, and eqn (2) fails badly. On the other hand as $\Phi_f(T) \rightarrow 0$, eqn (2) approaches eqn (1) as a limit. At values less than ~ 0.1 , however, the measurement of $\Phi_f(T)$ becomes experimentally difficult because of the low fluorescence intensities involved. At $\Phi_f(T) = 0.9$, eqn (2) underestimates the true activation energy by 79%, whereas at $\Phi_f(T) = 0.1$, the error is only 2%. Operationally, the use of eqn (2) to estimate activation energies works best for values of $\Phi_f(T)$ between approximately 0.1 and 0.3.

Other salient features

We observed hysteresis of fluorescence in samples that had been slowly heated and subsequently re-cooled to 10 °C (Fig. 7(a) and (b)). This could occur if $\Phi_f(T)$ is conformation-dependent, and/or if there is hypo- or hyperchromaticity in the coil relative to the helix. A review of collagen melting has been given by Privalov.²⁰ It is thought to be a slow, highly cooperative process in which the apparent T_m depends on the rate of heating. Hysteresis in collagen has been interpreted both in terms of an irreversible process (see¹⁰ and references therein) and as a reversible, but kinetically slow equilibrium.¹¹ Leikina *et al.*¹¹ demonstrated that the time it takes for complete collagen re-folding increases with increasing renaturation temperature. They found that at 28 °C, rat tendon type I collagen can take up to 10 days to renature; above 28 °C, renaturation did not occur.

We did not allow sufficient time for our re-cooled samples to completely re-fold, and therefore we cannot directly address this important issue. To minimize any complicating effects that might arise as a result of the slow re-folding kinetics, we incubated our collagen samples at 4 °C until use, prior to evaluating our thermodynamic data. We did not evaluate activation parameters from experiments in which the collagens were cooled from higher temperatures.

In view of these findings, it is evident that the conformation of the hairless mouse collagen allows for a greater degree of interaction between bound tyrosyl residues, than that of calf skin collagen. Moreover, our studies indicate that the structure and conformation of the collagen backbone has a palpable effect on the fluorescence spectra and temperature dependence of collagen-bound fluorophores. Once these phenomena are better understood, it is possible that they might be of use in determination of 3-dimensional supramolecular collagen scaffolding and structure in normal and pathological conditions.

Acknowledgements

Supported in part by NIH/MBRS Grant #08248 and RCMI Grant #RR03034. The author thanks Ms Abrienne M. Patta for her technical help.

References

- 1 J. M. Menter, G. D. Williamson, K. Carlyle, C. L. Moore and I. Willis, Photochemistry of type I acid-soluble calf skin collagen: Dependence on excitation wavelength, *Photochem. Photobiol.*, 1995, **62**, 402–408.
- 2 S. S. Lehrer and G. D. Fasman, Ultraviolet irradiation effects on poly-L-tyrosine and model compounds; Identification of bityrosine as a photoproduct, *Biochemistry*, 1967, **6**(3), 757–767.
- 3 A. J. Gross and I. W. Sizer, The oxidation of tyramine, tyrosine, and related compounds by peroxidase, *J. Biol. Chem.*, 1959, **234**(6), 1611–1614.
- 4 S. Sakura and D. Fujimoto, Absorption and fluorescence study of tyrosine-derived crosslinking amino acids from collagen, *Photochem. Photobiol.*, 1984, **40**(6), 731–734.
- 5 D. A. Malencik and S. R. Anderson, Fluorometric characterization of dityrosine: Complex formation with boric acid and borate ion, *Biochem. Biophys. Res. Commun.*, 1991, **178**(1), 60–67.
- 6 V. M. Monnier, R. R. Kohn and A. Cerami, Accelerated age-related browning of human collagen in diabetes mellitus, *Proc. Natl. Acad. Sci. U. S. A.*, 1984, **81**, 583–587.

-
- 7 B. J. Ortwerth, M. Prabhakaram, R. H. Nagaraj and M. Linetsky, The relative UV sensitizer activity of purified advanced glycation endproducts, *Photochem. Photobiol.*, 1997, **65**(4), 666–672.
 - 8 G. Beier and J. Engel, The renaturation of colluble collagen products formed at different temperatures, *Biochemistry*, 1966, **5**(8), 2744–2755.
 - 9 R. Consonni, L. Zetta, R. Longhi, L. Toma, G. Zanaboni and R. Tenni, Conformational analysis and stability of collagen peptides by CD and by ¹H- and ¹³C NMR spectroscopies, *Biopolymers*, 2000, **53**, 99–111.
 - 10 C. A. Miles, T. V. Burjanadze and A. J. Bailey, The kinetics of the thermal denaturation of collagen in unrestrained rat tail collagen determined by differential scanning calorimetry, *J. Mol. Biol.*, 1995, **245**, 437–446.
 - 11 E. Leikina, M. V. Merts, N. Kuznetova and S. Leikin, *Proc. Natl. Acad. Sci. U. S. A.*, 2002, **99**(3), 1314–1318.
 - 12 C. Seidel, A. Orth and K.-O. Greulich, Electronic effects on the fluorescence of tyrosine in small peptides, *Photochem. Photobiol.*, 1993, **58**, 178–184.
 - 13 F. W. J. Teale and G. Weber, Ultraviolet fluorescence of the aromatic amino acids, *Biochem. J.*, 1957, **65**, 476–482.
 - 14 L. H. Kligman and M. Gebre, Biochemical changes in hairless mouse skin collagen after chronic exposure to ultraviolet-A radiation, *Photochem. Photobiol.*, 1991, **46**, 367–378.
 - 15 N. D. Light, Collagen in skin-preparation and analysis, in *Methods in Skin Research*, ed. D. Skerrow and C. J. Skerrow, John Wiley and Sons, 1985, pp. 559–586.
 - 16 D. V. Bent and E. Hayon, Excited state chemistry of aromatic amino acids and related peptides I. Tyrosine, *J. Am. Chem. Soc.*, 1975, **97**, 2599–2606.
 - 17 S. Lindy, T. Sorsa, K. Suomolainen, A. Lauhio and H. Turto, Hyperchromic effect of collagen induced by human collagenase, *FEBS Lett.*, 1986, 1–4.
 - 18 E. J. Bowen and J. Sahu, The effect of temperature on fluorescence of solutions, *J. Phys. Chem.*, 1959, **63**, 4–7.
 - 19 A. L. Rubin, D. Pfahl, P. T. Speakman, P. F. Davison and F. O. Schmitt, Tropocollagen: Significance of protease-induced alterations. Denaturation, *Science*, 1963, **139**, 37–38.
 - 20 P. I. Privalov, Stability of Proteins. Proteins which do not present a single cooperative system, *Adv. Protein Chem.*, 1982, **35**, 1–104.